Assessing the Suitability of Multivariate Adaptive Regression Splines for Snow Cover Classification on Sentinel 2 MSI Data

[1,*] Semih Kuter [2,3] Zuhal Akyürek [4,5] Gerhard-Wilhelm Weber

[1]Cankiri Karatekin University, Forest Engineering Dept. Turkey [2]Middle East Technical University (METU), Civil Engineering Dept., Water Resources Lab, Turkey [3]METU, Geodetic and Geographic Information Technologies Dept., Turkey [4]Poznan University of Technology, Dept. of Marketing and Economic Engineering, Poland [5]METU, Institute of Applied Mathematics, Turkey

Main Motivation

Estimation of snow cover extent with high accuracy is of vital importance in order to have a comprehensive understanding for present and future climate, hydrological and ecological dynamics. Development of methodologies to obtain reliable snow cover information by means of optical *remote sensing* (RS) has long been one of the most active research topics of the RS community.

Supervised parametric *pixel-based classifiers* based on conventional Bayesian techniques such as *Maximum Likelihood* (ML) and *Minimum Distance* were the most frequently employed classification methods in RS until the mid-90s. In conjunction with rapid improvements in computer technologies and the development of new data mining methods in the areas of *Statistical Learning* and *Inverse Problems*, nonparametric *machine learning algorithms* have become increasingly popular for classification applications in RS since 90s.

Our main task in this study is to represent the utilization of *Multivariate Adaptive Regression Splines* (MARS) for snow cover classification on *ESA Sentinel 2 MSI* (cf. Figure 1) data. Three Sentinel 2 images acquired in Dec 2017, Mar 2018 and Apr 2018 over the northeastern part of Turkey are used as image dataset. Several spatial subsets taken from the images are classified by using both MARS and ML. The performances of MARS and ML algorithms are then assessed through the associated error matrices.

Figure 1. (a) Sentinel 2A being encapsulated, (b) Sentinel 2 MSI and (c) its global coverage.

Sentinel 2 MSI Instrument & Image Dataset Used in the Analysis

Sentinel 2 MSI is the name of two multispectral instruments, i.e., Sentinel 2A and 2B, developed and operated by ESA. The instrument has 13 spectral bands ranging from 442 to 2202 nm at three different spatial resolutions, i.e., 4 visible and near-infrared bands at 10 m, 6 red-edge/shortwave-infrared bands at 20 m, and 3 atmospheric correction bands at 60 m (cf. Table 1). Since the twin satellites are in the same sun-synchronous orbit with a phase delay of 180°, they guarantee an effective revisit time of 5 days at the equator and 2/3 days over mid-latitudes, with a 290-km swath width.

Since the modeling of snow-covered area in the mountainous regions of Eastern Turkey, as being one of the major headwaters of Euphrates–Tigris basin, has significant importance in order to forecast snowmelt discharge especially for energy production, flood control, irrigation and reservoir operation studies, three Sentinel 2 T37TFE tiles (cf. Figure 2) taken in 29 Dec 2017, 19 Mar 2018 and 8 Apr 2018 are selected as dataset.

Table 1. Designation of Sentinel 2 MSI bands.

Spectral Band	2A Central Wavelength (nm)	2B Central Wavelength (nm)	Spatial Resolution (m)
Band 1	442.7	442.2	60
Band 2	492.4	492.1	10
Band 3	559.8	559.0	10
Band 4	664.6	664.9	10
Band 5	704.1	703.8	20
Band 6	740.5	739.1	20
Band 7	782.8	779.7	20
Band 8	832.8	832.9	10
Band 8A	864.7	864.0	20
Band 9	945.1	943.2	60
Band 10	1373.5	1376.9	60
Band 11	1613.7	1610.4	20
Band 12	2202.4	2185.7	20

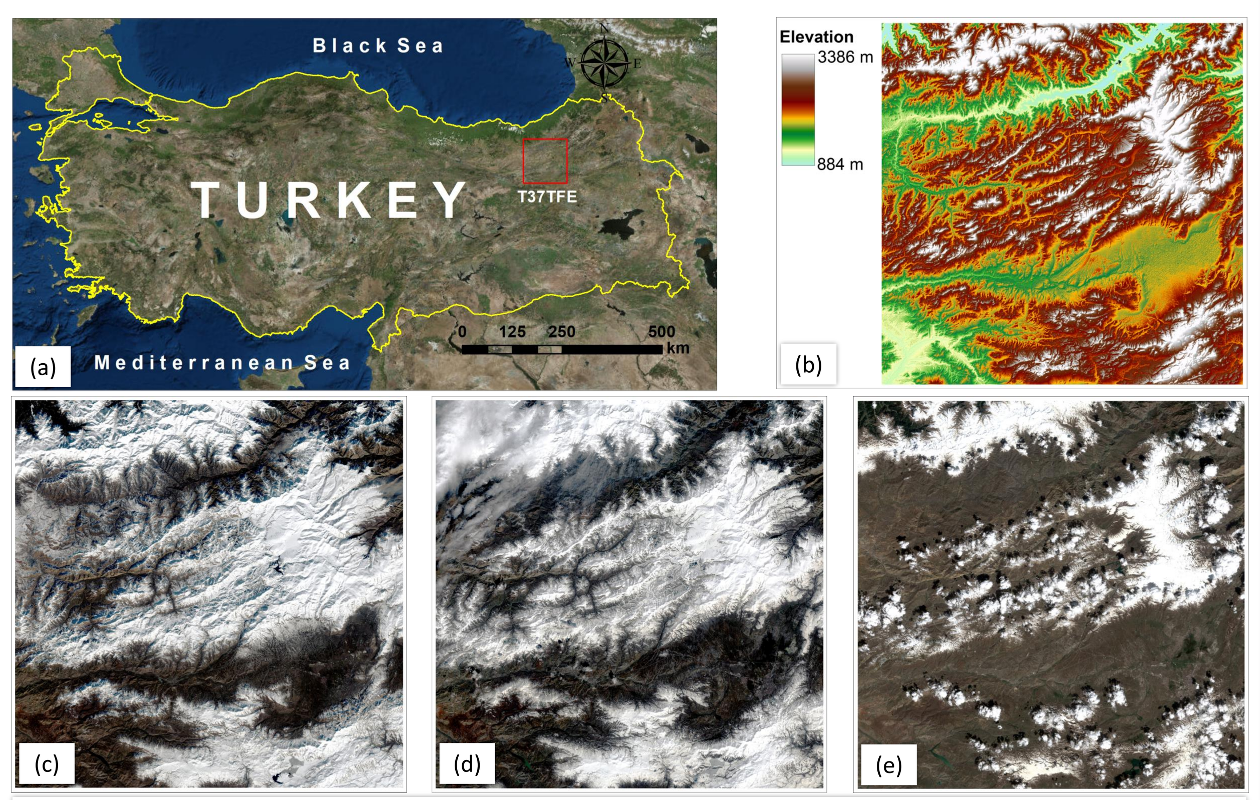

Figure 2. (a) Sentinel 2 T37TFE tile, (b) DEM, (c) RGB real-color images of Dec 2017, (d) Mar 2018, and (e) Apr 2018.

Scene Specific Conditions & Image Subsets

Dec 2017 image: There is no apparent cloud cover; therefore, class labels are decided as *ice*, *land*, *snow* and *water*; and two subsets of images are selected. **Mar 2018 image:** Three spatial subsets are taken. There exist cloud banks in the northwest quadrant and cumulus clouds in the southwest quadrant of the image. Additionally, several frozen water bodies are observed; thus, *cloud*, *ice*, *land*, *snow* and *water* are attained as class labels for this image. **Apr 2018 image:** Only one spatial subset is selected. In this image, there exists no frozen water bodies, and cumulus clouds are apparent over the whole scene; as a result, *cloud*, *land*, *snow* and *water* are chosen as class labels. Each spatial subset has size of 901 x 901 pixels (811,801 pixels in total), and they are shown in Figure 3.

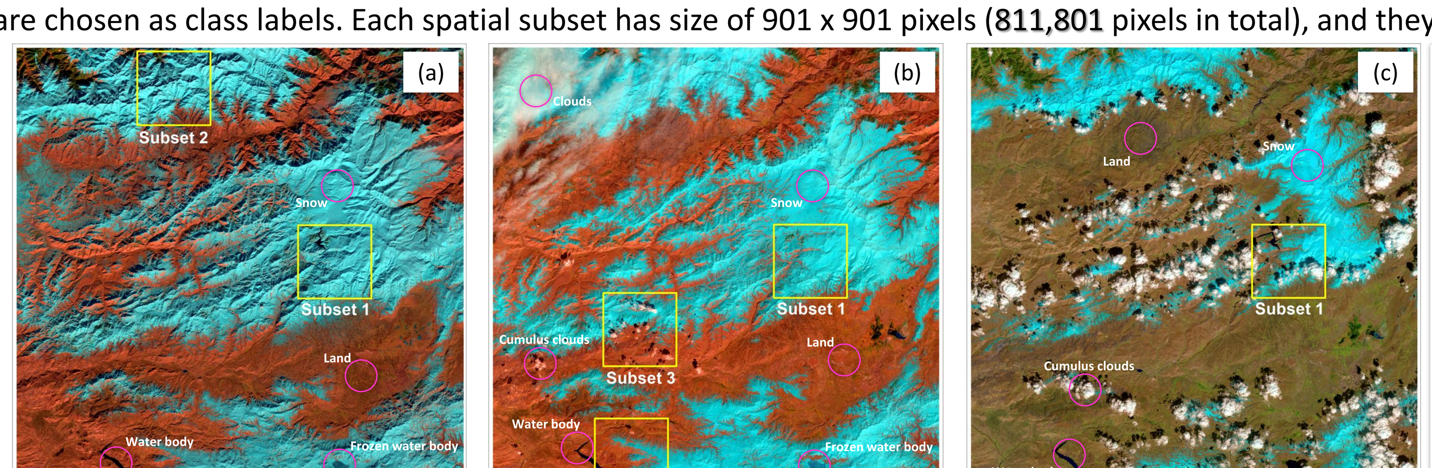

Figure 3. RGB false-color composite images of Sentinel 2 T37TFE tile for (a) Dec 2017, (b) Mar 2018, and (c) Apr 2018.
R: Sentinel 2 Band 11
G: Sentinel 2 Band 8A
B: Sentinel 2 Band 3
In this band combination, ice and snow appear as bright blue; whereas, water bodies are near black. Saturated soil can be seen also in blue, and clouds are still white.

MARS – Multivariate Adaptive Regression Splines

In MARS (Friedman, 1991), piecewise linear *Basis Functions* (BFs) are used in order to define relationships between a response variable and a set of predictors. These are "*linear splines*" and also known as "*reflected pair*" (cf. Figure 4). The range of each predictor variable is cut into subsets of the full range by using knots "τ" which defines an inflection point along the range of a predictor. BFs implied in MARS are expressed as follows (Hastie et al., 2009):

Basis Functions

$$[x-\tau]_+ = \begin{cases} x-\tau, & \text{if } x>\tau, \\ 0, & \text{otherwise,} \end{cases}$$

$$[\tau-x]_+ = \begin{cases} \tau-x, & \text{if } x<\tau, \\ 0, & \text{otherwise.} \end{cases}$$

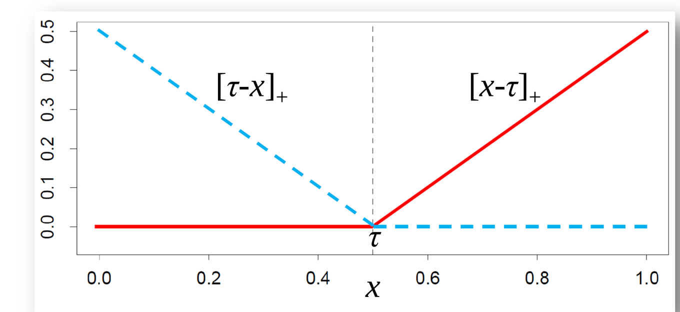

Figure 4. Truncated piecewise linear BF (i.e., reflected pair).

General Model

$$Y = f(\boldsymbol{X}) + \varepsilon$$

- Y: Response variable,
- $\boldsymbol{X} = (x_1, x_2, \ldots, x_p)^T$, vector of predictors,
- ε: observation error with zero mean and finite variance.

The set of 1-dimensional BFs of MARS

$$C := \left\{ [x_j-\tau]_+, \; [\tau-x_j]_+ \;\middle|\; \tau \in \{x_{1,j}, x_{2,j}, \ldots, x_{N,j}\} \right\}$$

Spline fitting in higher dimension by tensor products of univariate spline functions (cf. Figure 5)

Multivariate Spline BFs

$$B_m(\boldsymbol{X}^m) =: \prod_{j=1}^{K_m} \left[s_{\kappa_j^m} \cdot \left(x_{\kappa_j^m} - \tau_{\kappa_j^m} \right) \right]_+$$

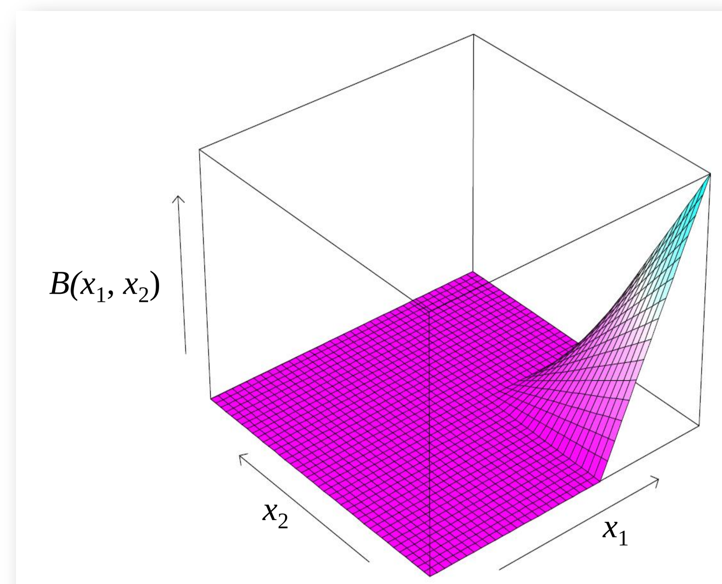

Figure 5. The function $B(x_1, x_2) = [x_1-\tau_1]_+ \cdot [\tau_2-x_2]_+$ generated by the multiplication of two piecewise linear BFs of MARS (Hastie et al., 2009).

MARS Model Function

$$Y = \beta_0 + \sum_{m=1}^{M} \beta_m B_m(\boldsymbol{X}^m) + \varepsilon$$

Estimation of model function $f(\boldsymbol{X})$

1st stage: Forward Pass
Large model that overfits the data

2nd stage: Backward Pass
Prune it without degrading the fit

By minimizing

Generalized Cross Validation

$$GCV(\alpha) := \frac{\sum_{i=1}^{N} \left(y_i - \hat{f}_\alpha(\boldsymbol{X}_i) \right)^2}{\left(1 - Q(\alpha)/N\right)^2}$$

- N: Total no. of observations,
- $j \in \{1,2,\ldots,p\}$,
- p: dimension of input space,
- K_m: Total no. of truncated linear functions multiplied in the m^{th} BF,
- $x_{\kappa_j^m}$: Input variable of the k^{th} truncated linear function in the m^{th} BF,
- $\tau_{\kappa_j^m}$: knot value for $x_{\kappa_j^m}$,
- $s_{\kappa_j^m} \in \{\pm 1\}$,
- $Q(\alpha) = u + dK$,
- K: no. of knots in Forward Pass,
- u: no. of linearly independent functions,
- d: cost for each BF optimization.

MARS algorithm can be modified to handle *multi-response* problems, i.e., *classification* tasks. In this approach, the response, *Y*, has ***k*** columns and the MARS algorithm generates ***k*** simultaneous models (Hastie et al., 2009).

Training & Testing of the Models

Images are resampled to 20 m by using Sentinel 2's own scene processing module Sen2Cor v2.5.5. TOA reflectance values of Sentinel 2 **bands 2-7**, band **8A**, **11** and **12**, as well as two auxilary variables directly derived from these bands, namely, *Normalized Difference Snow Index* (NDSI) and *Normalized Difference Water Index* (NDWI), are used as predictor variables (i.e., 11 predictors in total). Two basic MARS parameters to control the "*model tuning*" process: 1) *maximum allowed numbers of BFs in the forward pass* (max_BFs), 2) *maximum allowed degree of interactions between predictor variables* (max_INT).

Table 2. Number of pixels taken from each image for the training and the testing of MARS and ML algorithms.

29 December 2017		
Class Label	Training	Test
Ice	2,434	362
Land	19,313	1,039
Snow	12,102	1,136
Water	3,169	542
TOTAL	**37,018**	**3,079**

19 March 2018		
Class Label	Training	Test
Cloud	10,255	786
Ice	2,466	620
Land	12,893	1,744
Snow	12,621	1,827
Water	2,325	675
TOTAL	**40,560**	**5,652**

8 April 2018		
Class Label	Training	Test
Cloud	8,196	757
Land	13,265	534
Snow	6,268	568
Water	2,568	594
TOTAL	**30,297**	**2,453**

max_INT = {1, 2, 3}
max_BF = {5, 10, 15,..., 200}

$$\mathrm{NDSI}_{\text{Sentinel 2}} = \frac{\text{Band 3-Band 11}}{\text{Band 3+Band 11}}$$

$$\mathrm{NDWI}_{\text{Sentinel 2}} = \frac{\text{Band 3-Band 8A}}{\text{Band 3+Band 8A}}$$

MARS & ML Classification Results

Table 3. Error matrices for MARS and ML classifications.

Dec 2017

MARS (True Class \ Predicted Class)	Ice	Land	Snow	Water	Row Total
Ice	112	0	250	0	362
Land	0	1032	0	7	1039
Snow	0	0	1136	0	1136
Water	0	0	0	542	542
Column Total	112	1032	1386	549	3079

ML (True Class \ Predicted Class)	Ice	Land	Snow	Water	Row Total
Ice	35	0	327	0	362
Land	0	992	47	0	1039
Snow	0	0	1136	0	1136
Water	0	435	0	107	542
Column Total	35	1427	1510	107	3079

Mar 2018

MARS (True Class \ Predicted Class)	Cloud	Ice	Land	Snow	Water	Row Total
Cloud	753	0	29	4	0	786
Ice	0	0	0	620	0	620
Land	0	0	1744	0	0	1744
Snow	8	15	28	1776	0	1827
Water	0	0	0	0	675	675
Column Total	761	15	1801	2400	675	5652

ML (True Class \ Predicted Class)	Cloud	Ice	Land	Snow	Water	Row Total
Cloud	715	0	71	0	0	786
Ice	0	0	0	620	0	620
Land	0	0	1744	0	0	1744
Snow	0	22	190	1615	0	1827
Water	0	0	26	0	649	675
Column Total	715	22	2031	2235	649	5652

Apr 2018

MARS (True Class \ Predicted Class)	Cloud	Land	Snow	Water	Row Total
Cloud	757	0	0	0	757
Land	0	534	0	0	534
Snow	0	0	568	0	568
Water	0	0	0	594	594
Column Total	757	534	568	594	2453

ML (True Class \ Predicted Class)	Cloud	Land	Snow	Water	Row Total
Cloud	757	0	0	0	757
Land	0	534	0	0	534
Snow	0	60	508	0	568
Water	0	82	0	512	594
Column Total	757	676	508	512	2453

The Best MARS Model Settings

Dec 2017
max_INT = 1, max_BF = 30
OA = 91.7%

Mar 2018
max_INT = 1, max_BF = 55
OA = 87.5%

Apr 2018
max_INT = 1, max_BF = 10
OA = 100%

MARS & ML Classification Results (cont.)

The basic classification accuracy metrics are derived from the related error matrices given in Table 3. The *producer's accuracy* (PA), *user's accuracy* (UA) and *overall accuracy* (OA) values of both MARS and ML are shown in Figure 6. The performance of MARS models generated for each Sentinel 2 image with respect to max_INT and max_BF are represented in Figure 7.

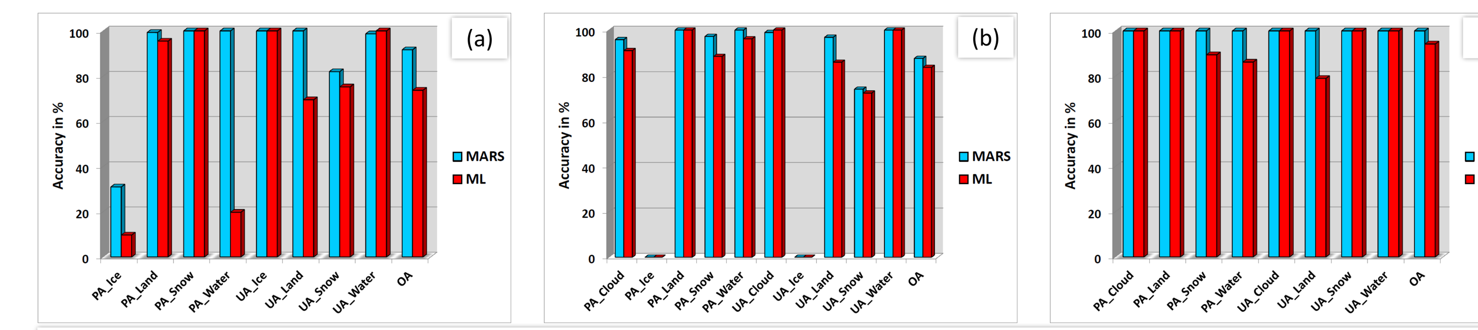

Figure 6. Basic classification accuracy metrics for (a) Dec 2017, (b) Mar 2018 and (c) Apr 2018 images.

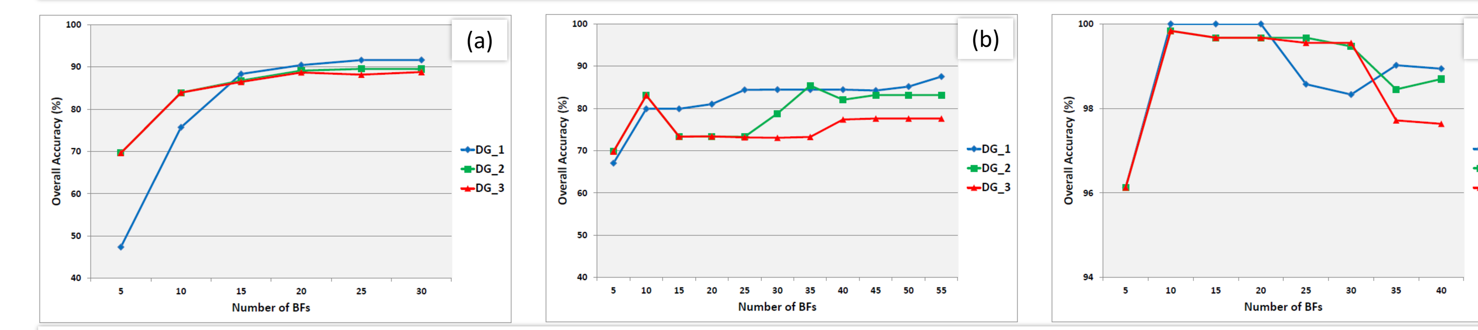

Figure 7. Overall accuracy of MARS models with respect to various max_INT and max_BF settings: (a) Dec 2017, (b) Mar 2018 and (c) Apr 2018.

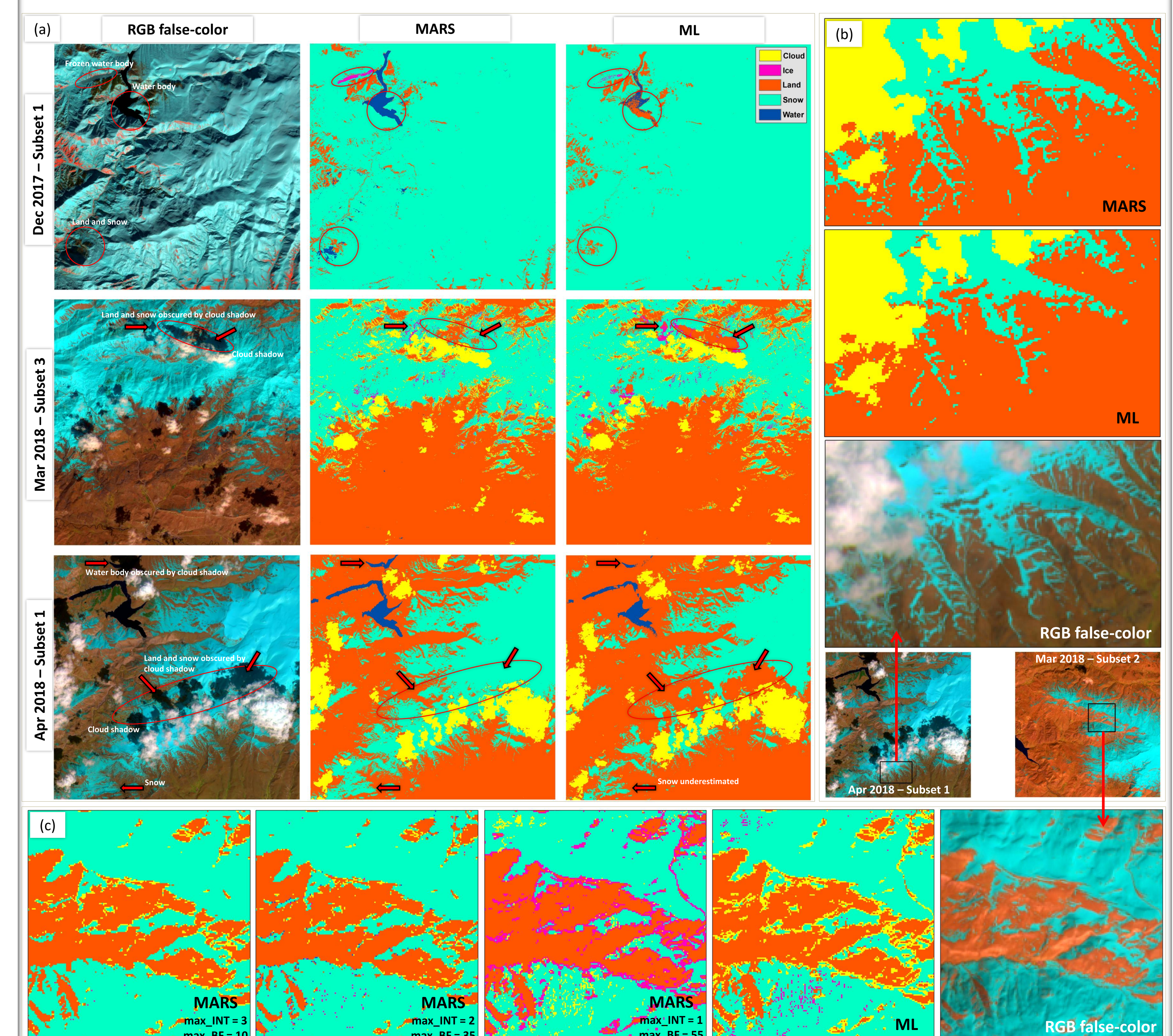

Figure 8. (a) The resultant classified images generated by MARS and ML, (b) Close-up view of April 2018 – Subset 1 image: The snow classification performance of MARS and ML, (c) Close-up view of March 2018 – Subset 2 image: Misclassification of snow as cloud at the snow-land boundary.

- *Ice-Snow misclassification*: As visually interpreted from Dec 2017 image in Figure 8-a, misclassification of ice occurs in both MARS and ML; however, MARS performance in resolving the confusion between ice and snow classes is much better than the ML's.
- *Land features obscured by cloud shadows*: As seen in both Mar and Apr 2018 images in Figure 8-a, MARS overperforms in correctly labeling land, snow and water features obscured by cloud shadows.
- *Under-/over-estimation of cloud and snow*: ML overestimates clouds at the cloud-snow boundary and underestimates snow at the land-snow boundary (cf. Figure 8-a Apr 2018 Subset 1 image & Figure 8-b).
- *Misclassification of wet and patchy snow*: The rate of mislabeling of wet and patchy snow as cloud at the land-snow boundary is higher for ML; whereas, MARS performance on this issue seems much better and increases with higher degree of interactions between predictor variables, i.e., max_INT (cf. Figure 8-c).

European Geosciences Union General Assembly 2019 (EGU 2019), 7-12 April 2019, Vienna, Austria (HS2.1.2 Snow and ice accumulation, melt, and runoff generation in catchment hydrology: Monitoring and modelling)

- **Friedman, J.H. (1991)**. Multivariate adaptive regression splines. *The Annals of Statistics, 19, 1-67.*
- **Hastie, T., Tibshirani, R., & Friedman, J. (2009)**. *The Elements of Statistical Learning: Data Mining, Inference, and Prediction. (2nd ed.). NY, USA: Springer.*

[1,*]semihkuter@karatekin.edu.tr; [2,3]zakyurek@metu.edu.tr; [4,5]gerhard.weber@put.poznan.pl